Elimination of Stress-Induced Curvature in Thin-Film Structures

Thomas G. Bifano, Harley T. Johnson, Paul Bierden, and Raji Krishnamoorthy Mali

Abstract—Argon ion machining of released thin-film devices is shown to alter the contour shape of free-standing thin-film structures by affecting their through-thickness stress distributions. In experiments conduffcted on MEMS thin-film mirrors it is demonstrated that post-release out-of-plane deformation of such structures can be reduced using this ion beam machining method. In doing so optically flat surfaces (curvature < 0.001 mm^{-1}) are achieved on a number of 3 μm-thick surface micromachined silicon structures, including mirrors with either initially positive curvature or initially negative curvature measuring up to 0.02 mm^{-1}. An analytical model incorporating the relevant mechanics of the problem is formulated and used to provide an understanding of the mechanisms behind the planarization process based on ion machining. The principal mechanisms identified are 1) amorphization of a thin surface layer due to ion beam exposure and 2) gradual removal of stressed material by continued exposure to the ion beam. Curvature history predictions based on these mechanisms compare well with experimental observations. [670]

I. INTRODUCTION

I N the decades since electronic thin-film fabrication techniques were first used to produce microelectromechanical systems (MEMS), significant progress has been made in modifying MEMS manufacturing processes to reduce film stresses and stress gradients. As a result of this progress, out-of-plane deformation of free-standing micromachined films can be limited to a level sufficient for many types of electromechanical sensors and actuators.

However, the recent, rapid emergence of micro*opto*electromechanical systems (MOEMS), which frequently require nanometer scale control of thin-film shape, has once again focused attention on the problem of stress and strain control in microfabrication. MOEMS devices frequently employ free-standing thin-film structures to reflect or diffract light. Stress-induced out-of-plane deformation must be small in comparison to the optical wavelength of interest to avoid compromising device performance.

A principal source of contour errors in micromachined structures is residual strain that results from thin-film fabrication and structural release. Surface micromachined films are deposited

T. G. Bifano is with the Manufacturing Engineering Department, Boston University, Brookline, MA 02446 USA (e-mail: tgb@bu.edu).

H. T. Johnson is with the Mechanical and Industrial Engineering Department, University of Illinois at Urbana-Champaign, Urbana IL 61801 USA.

P. Bierden is with the Boston Micromachines Corporation, Boston, MA 02472 USA.

R. K. Mali is with the Standard MEMS Corporation, Shelton, CT USA.

at temperatures significantly above ambient and they are frequently doped to improve their electrical conductivity. Both processes impose residual stresses in fabricated thin films. When sacrificial layers of the device are dissolved, residual stresses in the elastic structural layers are partially relieved by deformation of the structural layers. The extent of deformation is strongly dependent on process details and on the micromachined structure's geometry. Stress gradients through the thickness of a micromachined film are particularly troublesome from an optical standpoint, because they can cause significant curvature of a free-standing thin-film structure even when the average stress through the thickness of the film is zero.

The relationship between stress and curvature in thin-film structures is an active area of research, both for the development of MEMS technology and for the fundamental science of film growth. Vinci and Vlassak (1996) [1] review optical and microscopic techniques for measuring stress in thin uniform films on thick substrates by detecting wafer curvature. These methods rely on a model for the relationship between the wafer curvature and the stress in the film, proposed by Stoney (1909) [2], which is accurate for a class of systems meeting several important assumptions. Despite the fact that most MEMS thin-film applications of interest fall outside the class of problems for which Stoney's equation is applicable, most methods for inferring stress in the structures are still based on curvature or deflection measurements. Some models are available for these systems; Fang and Wickert (1996) [3] make some simplifications to determine the approximate stress and stress gradients in micromachined MEMS structures using curvature measurements, for example.

Some work has also been done to exploit or engineer the stress distributions in free-standing thin-film MEMS structures for application purposes. Yuan *et al.* (1992) [4] outline a method to obtain MEMS optical devices with desired curvature built-in, due to stress. Nowack *et al.* (1997) [5] attempt to reduce stresses in a thin-film/substrate system by means of ion bombardment; they attribute this effect to softening of the film material. Johnson and Krulevitch (1993) [6]discuss microstructural effects in stressed thin films and investigate stress gradients using a method of successive material removal.

In this paper, an approach to measurement and modification of residual stress gradients using ion beams is introduced. It will be shown that models of residual stress can be combined with such stress modification technique to allow localized measurement of residual stress gradients. Further, it will be shown that that ion beams can be employed to control of thin-film curvature by modifying the stress gradient through the thickness of the film.

II. THEORY-BASED UNDERSTANDING OF THE PROCESS

The measurement and modification approach described here is based on an analytical understanding of curvature of the structure in which processing and post-processing effects are viewed as sources of elastic mismatch strain. Using a model based on the work of Freund (1996) [7], the curvature of the free-standing structure can be predicted. The analysis is based on the work of Freund because it provides the most general possible framework in which arbitrary strain gradient distributions can be mapped into thin film out-of-plane deformation. As a result, particular mechanisms by which ion beam machining planarizes curved free-standing thin-film structures can be identified. The approach focuses on the relationship between the through-thickness mismatch *strain* distribution and the overall film curvature. Should the exact through-thickness *stress* distribution be of interest, as it is in Stoney equation based analyzes, it can be obtained from the material constitutive behavior of the film.

The thin-film device under consideration is a free standing square plate-like structure, on the order of several microns in thickness and several hundred microns in edge length, anchored to a silicon substrate by a narrow polycrystalline silicon post at the geometric center of the plate. The structure is fabricated using the well-known Cronos Multi-User Micromachining Process (MUMPS). This process involves the chemical vapor deposition and lithographic patterning of multiple polycrystalline Silicon layers and the deposition of several layers of phosphor-silica glass (PSG). The PSG layers are used as solid sources for diffusion doping; after phosphorus has been implanted in the silicon, the layers are removed, leaving the released and curved traction-free thin-film structure, shown in Fig. 1 (not to scale). Then, as a post-release step, a chemically neutral argon ion beam is used to alter the curvature of the film. For the purposes of analysis, both the diffusion and the ion beam exposure are viewed as contributions to an overall mismatch strain distribution $\varepsilon(z)$ in the film. The resulting curvature of the free-standing structure is then expressed analytically as a function of the strain distribution. A coordinate system is introduced whereby the bottom plane of the free-standing film is the origin of the z axis and the x and y axes are aligned with the plane of the film. The bottom and top surfaces of the film, at $z = 0$ and $z = h$ respectively, are assumed to be free of traction and the lateral edges are assumed to have no effect on the strain or curvature of the film. The mismatch strain distribution $\varepsilon(z)$ represents the equal biaxial strain in the plane of the film required to restore the silicon to an undeformed state relative to a traction-free, unprocessed condition. The total strain field in the structure after it is structurally released is the sum of these process-induced mismatch strains $\varepsilon^m(z)$ *and* the strain due to the resulting curvature of the film $\varepsilon^c(z)$

$$\varepsilon(z) = \varepsilon^m(z) + \varepsilon^c(z) \quad \text{where} \quad \varepsilon^c(z) = -\kappa z + \varepsilon^r \quad (1)$$

where κ is the film curvature and ε^r is a reference level of strain at the bottom of the film. The strain in the film is related to the stress through linear elasticity, so that the stress is

$$\sigma(z) = \frac{E(z)}{1 - v^2} \varepsilon(z) \quad (2)$$
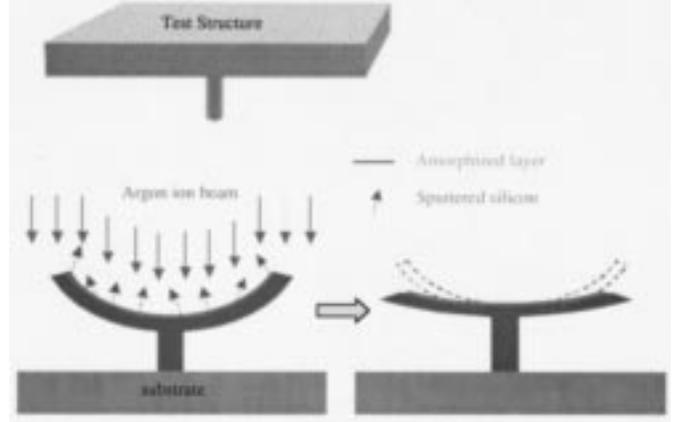

Fig. 1. Schematic of the test structure and the stress modification process: Accelerated argon ions bombard the upper surface of the free-standing thin-film structure, thereby modifying its residual stress gradient profile and changing its curvature. Surface amorphization and sputter etching are two ion-induced effects that alter the film stress.

where $E(z)$ is the elastic modulus, which may vary as a function of position (z) in the through-thickness direction. For the structures described above, structural release of the film relieves it of all external forces and moments, so that the equations of equilibrium in the film are

$$\int_0^h \sigma(z) = 0 \quad \text{and} \quad \int_0^h z\sigma(z)dz = 0. \quad (3)$$

Simultaneous solution of these equations yields an expression for curvature κ as a function of the process-induced mismatch strain $\varepsilon^m(z)$:

$$\kappa = \frac{-6}{h^2} \int_0^h \varepsilon^m(z)dz + \frac{12}{h^3} \int_0^h z\varepsilon^m(z)dz. \quad (4)$$

Thus, given knowledge of the processing mechanisms, from which an approximate strain distribution can be inferred, an overall curvature can be predicted. Comparing predicted curvatures to experimental data then allows an explanation of the diffusion and ion beam machining mechanisms, explained below. As an aside, (4) can be inverted so that, given a complete curvature history κ, recorded as a function of ion etch depth (z), the mismatch strain distribution $\varepsilon^m(z)$ and the original stress distribution in the thin film may be uniquely determined, assuming only that the biaxial stresses in the film are constant in the *in-plane* direction at a given height, z.

III. ION BEAM MACHINING PROCESS

The post-processing method for modifying thin-film curvature is broad beam neutral ion machining. In this process, depicted in Fig. 1, energetic, chemically neutral ions are accelerated toward the surface of a thin film in a uniformly distributed beam. Based on correlating to the analytical understanding of the process, it is asserted that, upon impact, the ion beam modifies the surface in two ways: first by disrupting the crystalline structure of the topmost layer of the film and then by slowly eroding the film in a sputter etching process. Removal of stresses embedded in etched layers changes the stress profile (and consequently, the contour shape) of the remaining film.

The system used in this work consists of a commercial broad beam Kaufmann ion source mounted in a vacuum chamber. Chemically neutral argon gas enters the source at a pressure of 0.2 mT. It is ionized by electrons emitted when current passes through a tungsten filament cathode in the source. These argon ions then migrate through a pair of closely spaced, charged grid plates, which accelerate them toward the sample holder. The argon ion beam emerges from a 110-mm grid plate at the front of the source and diverges to a diameter of 140 mm at the sample holder located 150 mm forward of the grid. Between the front of the source and the sample holder, a beam of electrons is entrained with the plasma. The electron beam current is matched to that of the argon ion beam, so that the plasma that arrives at the substrate is electrically neutral.

The kinetic energy dissipated as the argon ions collide with the surface of a sample is sufficient to break covalent atomic bonds in the sample. Under the steady impact of a beam then, the sample is first atomically disrupted (amorphized) and then material is removed (i.e., sputtered) at an approximately uniform rate. Length scales and rates of these processes depend on experimental conditions and can be found by correlating experimental results with the analytical model.

For the system used in this work, the argon beam was accelerated by grids biased at -500 V. The beam current density emerging from the source was 10 μA/mm^2. Under these conditions, the sputter etch rate for a polycrystalline silicon sample oriented with its surface perpendicular to the ion beam was found to average approximately 4 nm/min. The amorphized region is approximately 10 nm in depth. For these conditions, the beam's current flux density was found to be temporally and spatially uniform to within 5% over the area of the 120 mm diameter sample holder.

IV. ION BEAM MACHINING EXPERIMENTAL RESULTS

A number of silicon test mirrors measuring 200–400-μm square and 3.0–3.5-μm thick were fabricated in two different two level surface micromachining processes at Cronos Integrated Technologies. All of the 3.5-μm structures were fabricated using a structural composite of two polycrystalline silicon layers (Poly1 and Poly2) in Cronos MUMPS. The 2.0-μm-thick Poly 1 layer was deposited by low pressure chemical vapor deposition (LPCVD) on top of a patterned 2.0-μm-thick layer of phosphosilicate glass (PSG). This was followed by LPCVD deposition of a 200-nm-thick layer of PSG on top of Poly1 and a subsequent anneal at 1050 °C for one hour in argon. The anneal dopes the polysilicon with phosphorus from PSG layers above and below it and also thermally relieves some of the internal stresses in the as-deposited polysilicon film. The Poly1 layer was then patterned and etched. A second, 1.5-μm-thick polysilicon film (Poly2) was deposited on Poly1 using the same LPCVD process, again topped by a 200-nm layer of PSG and another anneal at 1050 °C for one hour in argon.

An important difference between the Poly1 and Poly2 processing was that Poly2 was annealed with PSG above, but not below the film (since the film was deposited directly on Poly1). All of the 3.0 μm structures were fabricated using a single polycrystalline silicon layer in a process similar to MUMPS Poly1, but with a thicker film produced by lengthening the LPCVD
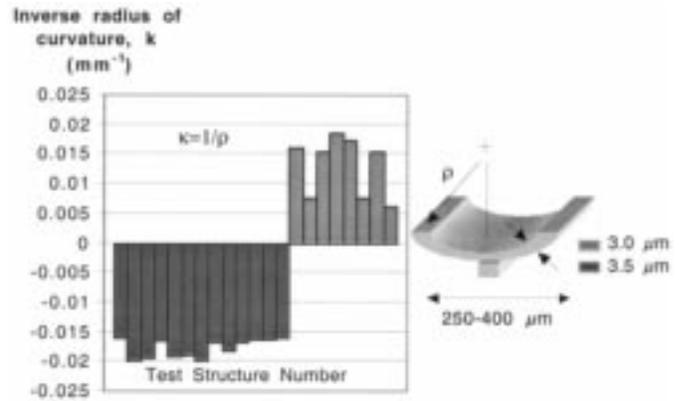

Fig. 2. Measured initial curvature (best fit) for 21 free-standing silicon test structures. The 3.5-μm structures consist of a composite silicon film (a sandwich of 2-μm-thick Poly 1 and 1.5-μm-thick Poly 2) produced through the Cronos MUMPS process. As fabricated, these exhibited convex curvature. The 3.0-μm-thick structures consist of a monolithic polycyrstalline silicon film, produced through a custom fabrication process at Cronos. As fabricated, these exhibited concave curvature.

deposition time. This custom process was developed for micromirror systems and has been described previously by Bifano (1999) [8]. Though it is possible to modify the deposition and annealing processes to reduce or eliminate out-of-plane deformation due to residual strain gradients, it is difficult to do so predictively to a level sufficient for production of optical components in surface micromachining processes.

All test mirrors were square plates supported by narrow (20 μm) square post attachments at their center. After structural release, each was ion machined in a custom designed etching chamber (Prism Corporation PSM 2000) using a broad beam Kaufmann ion source, exposing the test mirror to a flux of argon ions amounting to 10 μA/mm^2, accelerated by a 500 Volt potential. Before ion machining and at regular intervals during ion machining, the mirror surface shape was measured using an interferometric contour mapping microscope (WYKO NT2000).

Fig. 2 is a graph of the distribution of as-fabricated mirror shapes for the thirteen 3.5-μm-thick (composite) test structures and the eight 3.0-μm-thick (single layer) test structures studied. All samples exhibited contour shapes that closely approximated spherical sections. The 3.5-μm-thick structures were all initially convex, with an average radius of curvature $\rho = 52$ mm. The 3.0-μm-thick structures were all initially concave, with an average radius of curvature $\rho = 79$ mm. (The sign convention used in this work assigns negative curvature values to convex structures and positive curvature values to concave structures.) A more convenient way to quantify the contour shape of these structures is by their *inverse* radius of curvature, κ, since perfect flatness corresponds to $\kappa = 0$.

Even the flattest of these structures exhibits significant contour error relative to the wavelength of visible light and would be unacceptable as a mirror in many optical applications (e.g., optical cross-connectors, laser scanners, or spatial light modulators). Curvature of 100 mm, for example, corresponds to sag of about 110 nm over the lateral distance from the mirror's center to its edge (for a 300 μm square mirror). Such an error significantly disturbs the optical wavefront and compromises optical performance of the mirror.
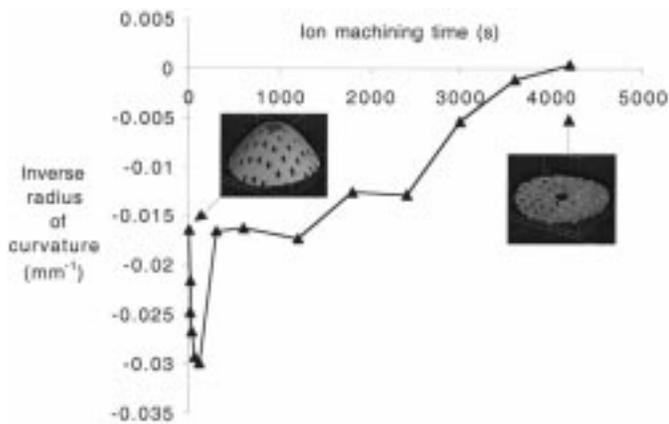
Fig. 3. Curvature as a function of ion machining time for an initially convex thin-film mirror segment measuring 300 μm on a side. The ion beam initially introduced a thin compressive layer in the film, making it more convex. Continued etching resulted in gradual removal of highly stressed surface layers in the film, causing the mirror to become optically flat. Also shown in the figure are measured interferometric contour maps of mirror shape. The theoretically predicted curvature evolution based on a mismatch strain distribution inferred from physical considerations is consistent with experimental data.

The first free-standing test structure to be ion machined was a 3.5-μm thick initially convex due to fabrication stresses. Its radius of curvature measured -62 mm, as depicted in Fig. 3. In the experiment, the ion beam immediately (within the first few seconds) affects mirror curvature, driving it into a more convex shape due to compression of a thin (~ 5 nm) layer at the film surface as a result of exposure to the ion beam. The theory-based understanding of this initial effect is that the high energy beam transforms the atomic structure of the thin layer from a polycrystalline state to an amorphous state, lowering its density; this density change is interpreted as a mismatch strain in (4) which predicts the corresponding observed curvature change. After this initial effect, a more gradual change in membrane shape takes place with additional ion machining time, as stressed layers in the film are etched away. Surface roughness of the mirrors is unaffected by this process. Ultimately the strain profile of the thin film is modified so that its curvature is entirely eliminated—yielding a nearly perfectly planar surface.

This test was repeated on the remaining twelve test structures and the results are depicted in Fig. 4, with different symbols corresponding to the different structures tested. (The black diamond data correspond to the test structure presented in Fig. 3.) All structures followed the same approximate path of curvature versus ion machining time, with an initial dip toward more negative curvature followed by a gradual shift toward more positive curvature.

Some devices were machined well beyond the time it took to make them flat and it can be seen in Fig. 4 that these test structures were transformed from convex to concave over the course of the experiment.

For all of these devices, a lengthy ion machining time was required to flatten the mirror by etching away the uppermost compressive surface. This long exposure to the ion beam can cause potentially significant damage to other parts of the MEMS device, including erosion of fast-etching metal films exposed to the beam and sputter redeposition of etched silicon on nearby structures. Both of these effects were observed in the long ion machining experiments.
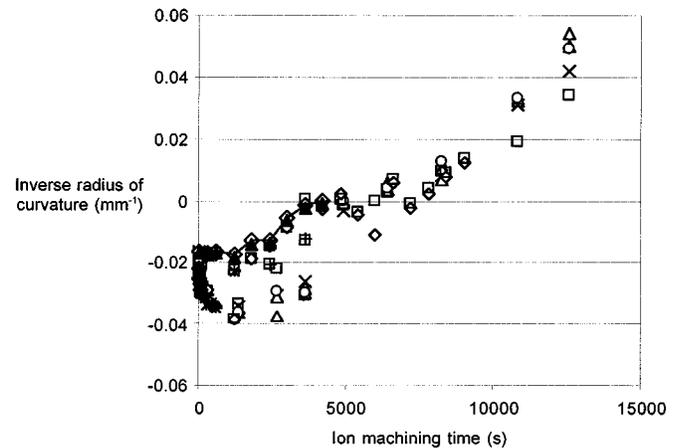

Fig. 4. Evolution of curvature as a function of ion machining time for the 3.5-μm-thick silicon test structures. The connected data points correspond to the structure detailed in Fig. 3.
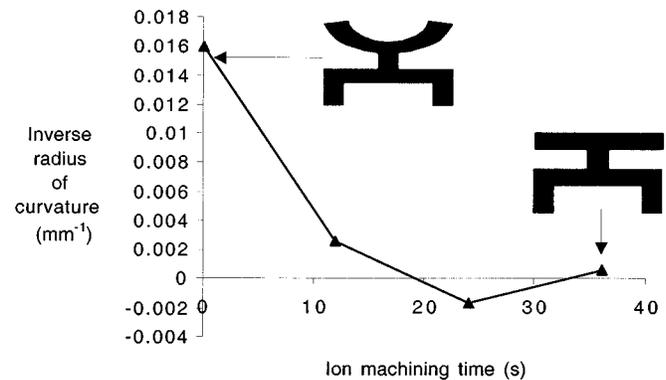

Fig. 5. A second test mirror, initially concave, was flattened in less than a minute of ion machining, through ion induced compression of its surface.

Rapid compression during initial ion machining (i.e., the initial decrease in inverse radius observed in Fig. 3) makes it possible to modify curvature of *concave* devices to near planar quality in a few tens of seconds, avoiding the previously described difficulties associated with long ion etching times. In fact, concave curvature is more common than convex in "as-fabricated" surface micromachined silicon thin films. Fig. 5 illustrates a remarkable confirmation of this rapid ion beam planarization process. An initially concave mirror test structure having curvature of $+60$ mm (inverse radius $+0.016$ mm^{-1}) was planarized to a radius of curvature of $+2$ meters (inverse radius $+0.0005$ mm^{-1}) in only 35 s of exposure to the ion beam.

This test was repeated on the remaining seven test structures and the results are depicted in Fig. 6, with different symbols corresponding to the different structures tested. (The black diamond data correspond to the test structure presented in Fig. 6). Each structure was transformed from concave to essentially flat over the course of 20–36 s of ion machining.

Because ion bombardment causes rapid microstructural changes in a thin layer of the film, it might be expected that these induced deformations would be partially reversed by diffusion over time or after exposure to elevated temperatures. Several tests were conducted on ion machined (and nonion machined) micromirrors to determine the effects of time and temperature on ion-induced changes in curvature. It was found
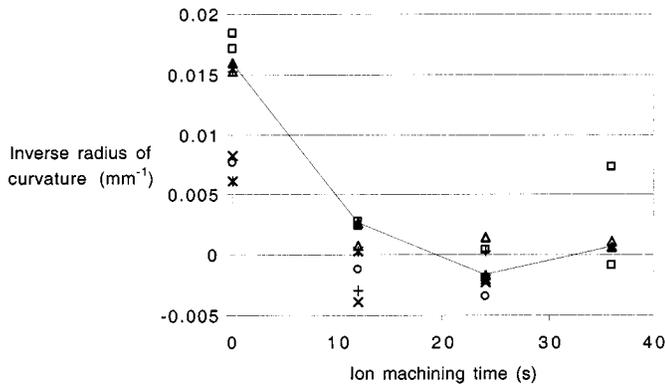
Fig. 6. Curvature evolution of eight 3.0-μm-thick free-standing silicon test structures, which were all initially concave, over 36 s of ion bombardment. Less than 10 nm of material was removed trough this process. The primary effect of the ion beam is to impose a compressive stress due to amorphization of a thin surface layer, changing the stress gradient profile and flattening the structure. The connected data points correspond to the structure detailed in Fig. 3.
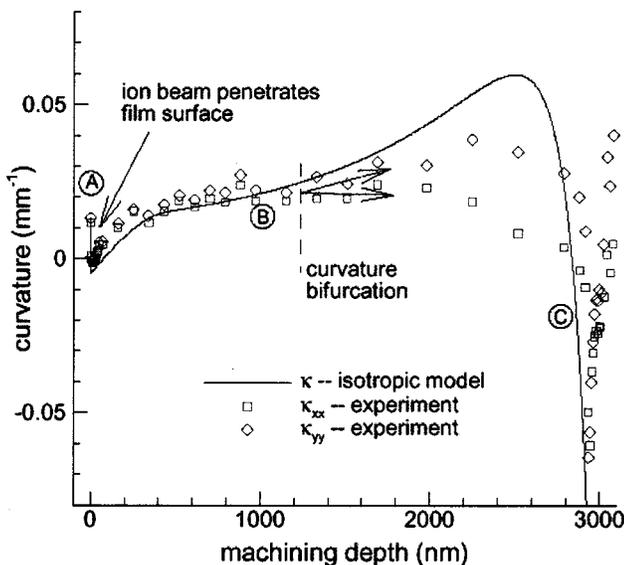

Fig. 7. Curvature history of a 3.0-μm-thick, initially concave silicon mirror etched almost completely through by an ion beam. Such a curvature history can be used to determine the original stress or strain profile in the film. In the figure, curvature data was recorded in two orthogonal directions in the plane of the mirror surface. The measured curvature becomes anisotropic approximately half way through the etching process. The red line corresponds to an analytical model prediction for the expected curvature. The model assumes a linear strain distribution on the top and bottom layers of the film, due to Phosphorus diffusion with a penetration depth of 400 nm. Ion beam induced strain is modeled as 1% (compressive) with a depth of 5 nm.

that ion-induced changes in inverse radius-of-curvature were relieved by up to 10% within 100 h ion machining for a number of samples. Subsequent heating to 100 °C for one hour resulted in no change in curvature. Tests conducted at higher temperatures after ion machining showed more significant effects, relieving up to one third of the ion induced change in inverse radius of curvature after 42 h at 200 °C.

In the final experiment, a silicon micromirror test structure was machined with the ion beam for an extended time, etching nearly all the way through the membrane (see Fig. 7). With this complete curvature history of the machined film, the parameters in the model for the mismatch strain can be precisely fit.

Also, the complete curvature history allows for the calculation of the through-thickness stress profile, through the inverted form of (4). Clearly, as shown in Fig. 7, the predicted curvature change closely follows the observed curvature change. This agreement provides strong support for the mechanisms of surface amorphization and stressed material removal postulated in the model.

V. DISCUSSION AND CONCLUSION

An analytical model is used to relate curvature to mismatch strain gradients resulting from the deposition, doping and annealing processes used in the manufacture of structural thin films. Based on insight provided by this model, a novel approach to modification of thin-film strain and curvature is developed. Broad-beam neutral ion beam machining is used to generate a thin layer of compressive strain at the film surface and to gradually etch the film from one side, removing layers of strained material. Through the combination of these two effects, both concave and convex free-standing structures are rendered optically flat. This is important for numerous optical MEMS devices including optical cross-connect switches, deformable mirrors and spatial light modulators, in which stress induced curvature large enough to compromise optical performance is often observed.

It is also shown that the curvature history of an ion beam machined, free-standing thin-film structure can be used to infer the original strain (or stress) profile in the film, providing a powerful tool for monitoring and evaluating MEMS fabrication processes. By combining (4) with the experimental data shown in Fig. 5, all of the curvature history information needed to *numerically* determine the through-thickness strain distribution and thus the stress distribution, is known. This technique allows for complete characterization of the stress condition of a free-standing MEMS structure.

The fundamental link in the theory relating stress and curvature in MEMS thin-film structures is that fabrication processes can be viewed as sources of mismatch strain. Then, through equilibrium, compatibility and material constitutive behavior, a relationship between through thickness mismatch strain distribution and overall curvature is derived. The relationship may be written as an expression for curvature as a function of mismatch strain, or inverted as an expression for mismatch strain as a function of curvature.

REFERENCES

[1] R. P. Vinci and J. J. Vlassak, "Mechanical behavior of thin flims," in *Annu. Rev. Mater. Sci. 26*: Annual Reviews Inc., 1996, pp. 431–462.
[2] G. G. Stoney, "The tension of metallic films deposited by electrolysis," *Proc. Royal Soc. London*, vol. A82, p. 172, 1909.
[3] W. Fang and J. A. Wickert, "Determining mean and gradient residual stresses in thin flims using micromachined cantilevers," *J. Micromechan. Microeng.*, vol. 6, no. 3, pp. 301–309, 1996.
[4] F. Yuan, Y. Shih, L. V. Knight, R. T. Perkins, and D. D. Allred, "Using thinflims to produce precision, figured X-ray optics," *Thin Solid Films*, vol. 220, no. 1–2, pp. 284–288, 1992.

[5] R. Nowack, Y. Miyagawa, C. L. Li, S. Nakao, S. Maruno, and S. Miyagawa, "Post-deposition reduction of internal stress in thin flims: The case of HfN coatings bombarded with Au ions," *Mater. Lett.*, vol. 33, no. 1–2, pp. 31–36, 1997.

[6] G. C. Johnson and P. Krulevitch, *Stress Gradients in Thin Flims Used in Micro-Electro-Mechanical Systems*: American Society of Mechanical Engineers, Dynamic Systems and Control Division, 1993, vol. 46, DSC, pp. 89–95.

[7] L. B. Freund, "Some elementary connections between curvature and mismatch strain in compositionally graded thin flims," *J. Mechan. Phys. Solids*, vol. 44, p. 723, 1996.

[8] T. G. Bifano, J. Perreault, R. K. Mali, and M. N. Horenstein, "Microelectromechanical deformable mirrors," *J. Select. Topics Quantum Electron.*, vol. 5, pp. 83–90, 1999.

Thomas G. Bifano received the B.S. and M.S. degrees in mechanical engineering and materials science from Duke University, Durham, NC, in 1980 and 1983, respectively, and the Ph.D. degree in mechanical engineering from the North Carolina State University, Raleigh, in 1988.

He has more than a decade of research experience in the field of precision optical engineering. His principal areas of expertise concern measurement, actuation and fabrication at the submicrometer tolerance level in optical applications. He has organized and chaired two international conferences for the American Society for Precision Engineering and recently served as a member of the board of directors for the society. He joined the College of Engineering at Boston University (BU), Brookline, MA, in 1988, where he now chairs the Manufacturing Engineering Department. He direct the Precision Optics Laboratory at the BU Photonics Center. His research at BU currently includes the development of micromechanical mirror arrays on a silicon chip, the development of new precision manufacturing technology for compact disk production and basic research on the design, fabrication, and control of new classes of smart materials.

Harley T. Johnson received the B.S. degree in engineering science and mechanics from Georgia Institute of Technology, Atlanta, in 1994, the M.S. degrees in engineering and applied mathematics and the Ph.D. degree in solid mechanics from Brown University, Providence, RI, in 1996, 1998, and 1999, respectively.

He is an Assistant Professor of Mechanical and Industrial Engineering at the University of Illinois at Urbana-Champaign. His research is in the area of micro- and nanomechanical effects in materials for electronic and optical applications. He has developed models and approaches for studying thin-film structures, semiconductor quantum devices, Microelectromechanical systems and photonic materials. Prior to joining the faculty at the University of Illinois, he was an Assistant Professor of Aerospace and Mechanical Engineering at Boston University, Boston, MA.

Dr. Johnson received a 2001 NSF CAREER development award for his work.

Paul Bierden received the B.S. and M.S. degree in mechanical engineering from Boston University, Boston, MA.

Currently, he is the President of Boston Micromachines, Boston, MA. He is currently PI on a number of DoD sponsored program to develop advanced MEMS for optical and fluidic systems. He has spent the last four years working with Prism Corporation as Chief Research Engineer. While at Prism, he was responsible for more than $1M in research and development funding. His principal efforts were directed toward demonstrating feasibility of a pioneering new approach to CD and DVD manufacturing methods, constructing a commercial prototype process and then transferring that technology to a production scale environment. He was responsible for technical research, liaison with industrial partners and development of new manufacturing technologies. While working for Prism, he played an integral part in Prism being awarded Phase I and Phase II STTR awards from the Department of Energy and successfully launched a Phase III program for commercialization. He brings to this project a strong background in material science, optics, semiconductor fabrication, and system integration.

Raji Krishnamoorthy Mali received the B.S. degree in mechanical engineering from the University of Bombay, India, in 1992. She was a Presidential University Graduate Fellow at Boston University, Boston, MA, and received the M.S. and Ph.D. degrees in mechanical engineering in 1994 and 1999, respectively. For her Ph.D. dissertation, she developed MEMS deformable mirrors for adaptive optics applications.

From 1998 to 2002, she worked as a MEMS development engineer from 1998-2002 with Standard MEMS, Inc., Hauppauge, NY, and Shelton, CT. She was involved in the design and development of various MEMS products, including optical devices, RF devices and various sensors. She is currently a Senior Engineer with D-Star Engineering Corporation, Shelton, CT, and develops MEMS components and subsystems for small engines and power systems.